

* · V. R. Sanal Kumar ** · ***

A Computational Study of the Supersonic Coherent Jet

Mi-Seon Jeong, V. R. Sanal Kumar and Heuy-Dong Kim

Key Words : Compressible Flow(), Combustion(), Shock Wave(), Supersonic Coherent Jet(), Entrainment Effect(), Potential Core Length()

Abstract

In steel-making process of iron and steel industry, the purity and quality of steel can be dependent on the amount of CO contained in the molten metal. Recently, the supersonic oxygen jet is being applied to the molten metal in the electric furnace and thus reduces the CO amount through the chemical reactions between the oxygen jet and molten metal, leading to a better quality of steel. In this application, the supersonic oxygen jet is limited in the distance over which the supersonic velocity is maintained. In order to get longer supersonic jet propagation into the molten metal, a supersonic coherent jet is suggested as one of the alternatives which are applicable to the electric furnace system. It has a flame around the conventional supersonic jet and thus the entrainment effect of the surrounding gas into the supersonic jet is reduced, leading to a longer propagation of the supersonic jet. In this regard, gasdynamics mechanism about why the combustion phenomenon surrounding the supersonic jet causes the jet core length to be longer is not yet clarified. The present study investigates the major characteristics of the supersonic coherent jet, compared with the conventional supersonic jet. A computational study is carried out to solve the compressible, axisymmetric Navier-Stokes equations. The computational results of the supersonic coherent jet are compared with the conventional supersonic jets.

1. 가 , , 3-5% 가 , (Barrel) (1-4) 가 가

*

E-mail : kimhd@andong.ac.kr
TEL : (054)820-5622 FAX : (054)823-5495

** PRG, Vikram Sarabhai Space Centre, India

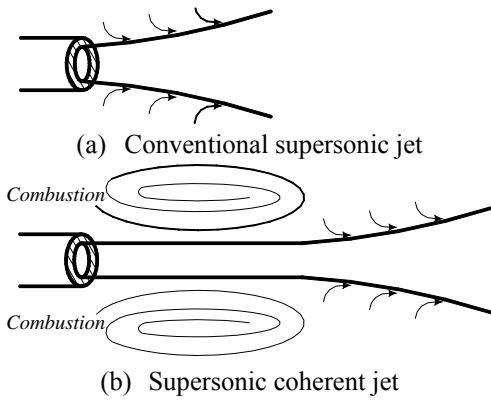


Fig. 1 Schematics of conventional supersonic jet and coherent jet

(5-8)

Fig.1

가

(coherent)

Fig.1 (a)

가

Fig.1 (b)

coherent (5-8)

coherent Brhel⁽⁹⁾

Mathur

가

가

가 coflow

(10)

2.

coherent

$k-\epsilon$
Navier-Stokes

$$\frac{\partial \rho}{\partial t} + \frac{\partial}{\partial x_i}(\rho u_i) = 0 \quad (1)$$

$$\frac{\partial}{\partial t}(\rho u_i) + \frac{\partial}{\partial x_j}(\rho u_i u_j) = \frac{\partial}{\partial x_j} \left[\mu \left(\frac{\partial u_i}{\partial x_j} + \frac{\partial u_j}{\partial x_i} \right) \right] \quad (2)$$

$$- \frac{\partial}{\partial x_i} \left(\frac{2}{3} \mu \frac{\partial u_i}{\partial x_i} \right) - \frac{\partial p}{\partial x_i} + \frac{\partial}{\partial x_j} \left(-\rho u_i u_j \right)$$

$$\frac{\partial}{\partial t}(\rho E) + \frac{\partial}{\partial x_i}(\rho u_i H) =$$

$$\frac{\partial}{\partial x_j} \left[\left(x + \frac{\mu_t}{Pr_t} \right) \frac{\partial T}{\partial x_i} + u_j (\tau_{ij})_{eff} \right] \quad (3)$$

4 Runge-Kutta

source

volumetric reactions

(Y_i)

$$\frac{\partial}{\partial t}(\rho Y_i) + \nabla \cdot (\rho \vec{v} Y_i) = -\nabla \cdot \vec{J}_i + R_i \quad (4)$$

R_i

i

()

\vec{J}_i

i

flux

R_i

Finite chemistry

\vec{J}_i

$$\vec{J}_i = - \left(-\rho D_{i,m} + \frac{\mu_t}{Sc_t} \right) \nabla Y_i$$

Sc_t

Schmidt number, $D_{i,m}$

i

$$\nabla \cdot \left[\sum_{i=1}^n h_i \vec{J}_i \right]$$

가

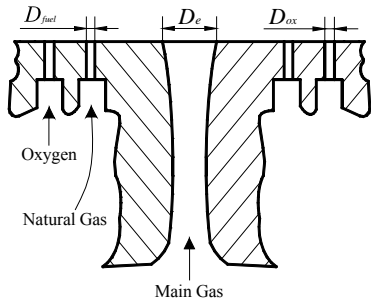
Lewis 가 1

gas

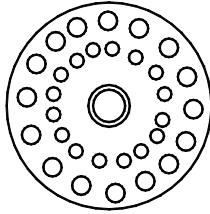
CH_4

O_2

Natural



(a) Coherent nozzle



(b) Cross sectional view the nozzle used in experiment

Fig. 2 Schematics of the supersonic coherent nozzle

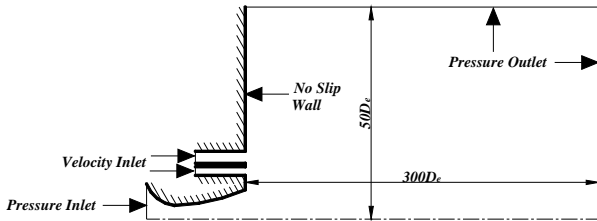


Fig. 3 Computational flow field and boundary conditions

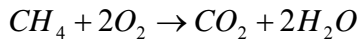


Fig.2

Fig.2 (a) (10) (D_e)

1.47cm, (throat) (D_t) 1.08cm
 (M_e) 가 2.1
 가

Natural gas Oxygen
 $D_{fuel} = 0.287\text{cm}, D_{Ox} = 0.408\text{cm}$

1200CFH 가 Fig.2 (b)

2
 가

3

Fig.3

$300D_e$
 $50D_e$

pressure inlet
 velocity inlet

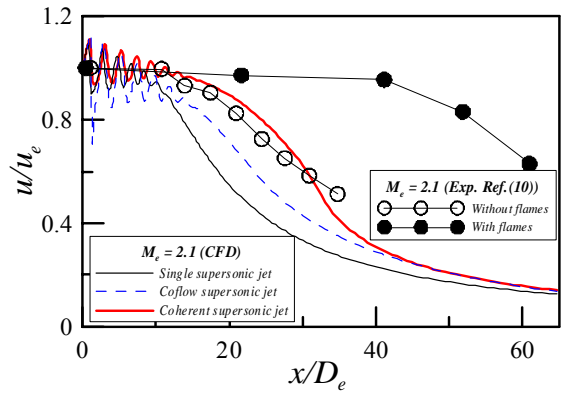


Fig. 4 Velocity distributions along the nozzle axis

pressure outlet
 no-slip
 implicit method
 explicit method
 Species-Transport
 Reactions
 Eddy-dissipation
 $k-\epsilon$
 10^{-4}
 0.5%
 가
 3.
 Fig.4 (10)
 $x/D_e =$
 12
 가 3.5
 가
 $x/D_e =$
 11
 가
 $x/D_e = 17$

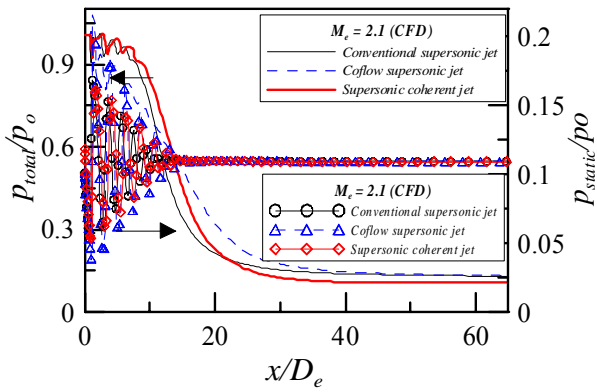


Fig. 5 Total and static pressure distributions along the nozzle axis

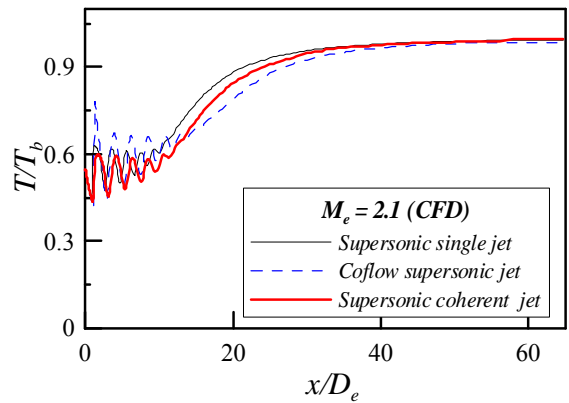


Fig. 6 Static temperature distributions along the nozzle axis

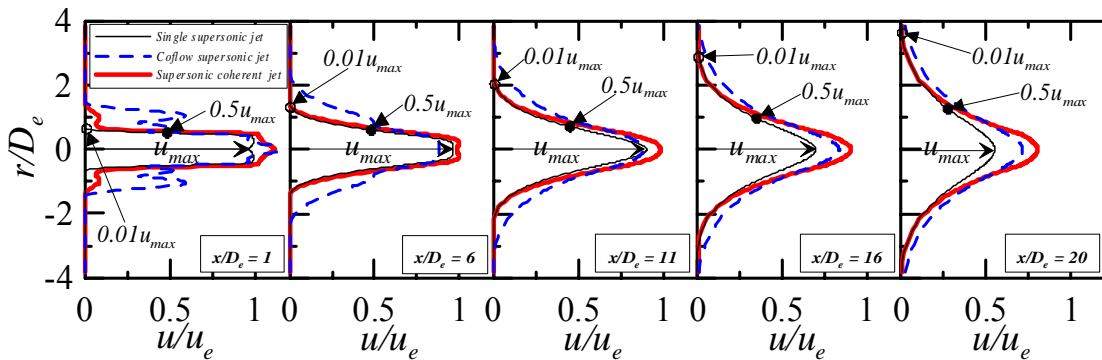


Fig. 7 Velocity distributions in the radial direction

x/D_e
 1.8 , 2 가 , coflow
 가 , 3 , $15 < x/D_e < 30$ coflow
 가 , 2 coherent 가
 Fig.5 Fig.7 x/D_e 가 1, 6, 11, 16,
 20
 $x/D_e = 10$,
 , coflow (potential core) 가
 가
 coherent , x/D_e 가 가 potential
 core
 1.5 가 가
 potential core ,
 Fig.6 가 가 coflow
 , $x/D_e = 6$ potential core
 (298K) 가
 x 가
 D_e , coflow 가
 가 가
 coflow coherent , coherent potential core
 x/D_e , $x/D_e = 16$

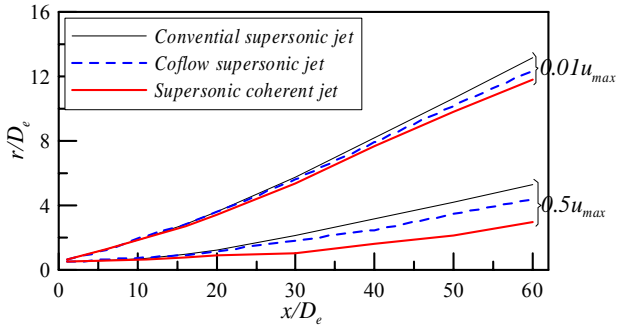


Fig. 8 Comparison of jet widths

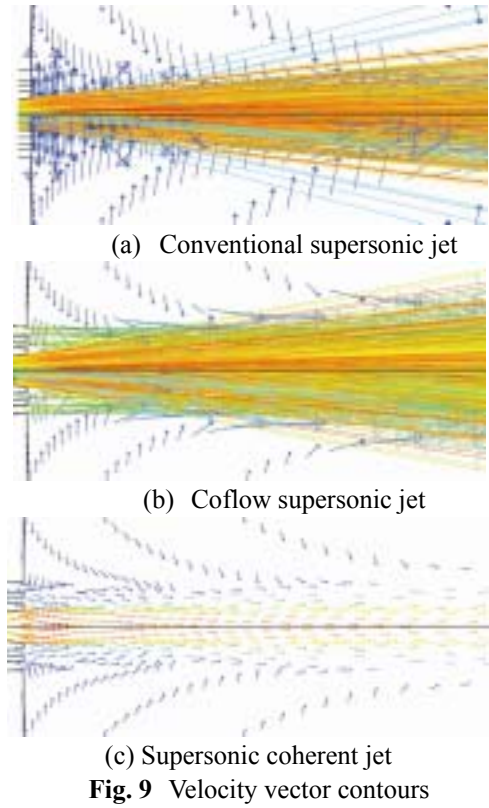


Fig. 9 Velocity vector contours

u_{max} , $0.5u_{max}$ 가
 $0.01u_{max}$ 가
 Fig.8
 x/D_e 가
 가
 $x/D_e = 25$ 가
 $x/D_e = 20$ 가
 r/D_e 가
 coflow 가
 coherent 가
 x/D_e 가
 Fig.9 가
 가
 (a) 가 , (b) 가
 coflow , (c) 가
 (a) ,
 가
 가
 (b) (a) ,
 $x/D_e > 16$

(c)
 coflow
 coherent
 가
 Fig.10
 x/D_e 가 1, 6, 11, 16,
 20
 $x/D_e = 1$ 가
 가
 coflow coherent
 가
 가
 coflow 가 coherent
 가 , $x/D_e = 6$,
 가 ,
 , $x/D_e > 16$
 0
 Table.1
 가
 \dot{m}_{in} ,
 $300D_e$

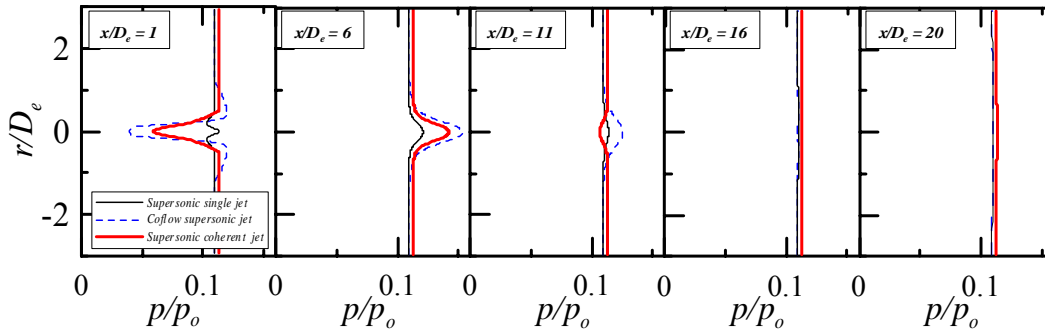


Fig. 10 Static pressure distributions in the radial direction

Table. 1 Comparison of mass entrainments

Jet	\dot{m}_{in}			\dot{m}_{out}	$\dot{m}_{out} / \dot{m}_{in}$
	\dot{m}_{jet}	\dot{m}_{fuel}	\dot{m}_{ox}		
Single	0.170	0	0	0.240	1.412
Coflow	0.170	0.092	0.197	0.569	1.240
Coherent	0.205	0.006	0.012	0.259	1.161

, coflow , coherent , coherent entrainment effect 가 가

2003

21

\dot{m}_{out}

entrainment

\dot{m}_{in} 40% , coflow

24%, coherent 16%

, coherent entrainment effect 가 가

4.

2

Navier-

Stokes

coherent

3

가

3

(1) coherent

1.8

(2)

potential core

가

coflow

coherent

x/D_e

, $x/D_e = 16$

(3)

coherent

가 가

(4)

가

- (1) Fox, J. H., 1974, "On the Structure of Jet Plumes," *J. AIAA*, Vol. 12, pp.105~107.
- (2) Hu, T. and McLaughlin, D., 1990, "Flow and Acoustic Properties of Low Reynolds number Underexpanded Supersonic Jets," *J. Sound and Vibration*, Vol. 141, pp.485~505.
- (3) Love, E. S., Grigsby, C. E., Lee, L. P. and Woodling, M. J., 1959, "Experimental and Theoretical Studies of Axisymmetric Free Jet," NASA TR R-6.
- (4) Amson, T. and Nicolls, J., 1959, "On the Structure of Jets from Highly Underexpanded Nozzles into still Air," *J. Aero space Science*, Jan., pp.16~24.
- (5) Mathur, P. C., Konicics, D. and Engle, D., 1997, "Results of Oxygen Injection in the EAF with Praxair Coherent Jet Injectors: A Novel Technology," *Electric Furnace Conference Proceedings, ISS*, Vol. 55, pp.305~313.
- (6) Busboom, E. Cooper, S. and Daubler, L., 1998, "Improving EAF Productivity with Praxair Coherent Jet Technology," *Electric Furnace Conference*, November.
- (7) Sarma, B. et al., 1998, "Fundamental Aspects of Coherent Gas Jets," *Electric Furnace Conference Proceedings, ISS*, Vol. 56, pp.657~672.
- (8) Anderson, J. E., Mathur, P. C. and Selines, R. J., 1998, "Method and Introducing Gas into a Liquid," U.S. Patent No.5814125, September.
- (9) Brhel, J., Shver, V., Coburn, M., Blakemore, R. and Mendrek, A., 2001, "An Improved Method of Applying Chemical Energy into the EAF," *Air Products and Chemicals, Inc.*
- (10) Anderson, J. E., Sommers, N. Y., Farrenkopf, D. R. and Bethal, Conn., 1998, "Coherent Gas Jet," U.S. Patent No.5823762, Oct.